

Tidal currents assessment in the Lima estuary

Illina S. Cândido Rebordão¹

¹ Department of Civil Engineering, Instituto Superior Técnico,

Technical University of Lisbon,

Av. Rovisco Pais 1049-001, Lisboa, Portugal

Abstract

The present study comprised an application of a hydrodynamic model for the Lima estuary and a basic assessment of tidal current energy. The calibration phase of the model consisted in choosing the best parameters in order to obtain results which are more consistent with the observed data. The numerical model ADCIRC was used and the wetting/drying tool was applied. This led to new results that were compared with previous values from a study that did not use this tool. The importance of the wetting/drying in this domain was evaluated.

A short description of the main features and requirements of the present tidal energy technology and an evaluation of the tidal conditions in the estuary allowed the assessment of the feasibility for the installation of equipment to produce energy using the tidal fluxes in the Lima estuary.

Keywords: ADCIRC, hydrodynamic modelling, Lima estuary, tides, tidal current energy, wetting/drying.

Introduction

The urge to exploit alternative and clean energy sources has motivated the development of new technology. The ocean environment has many energy resources. Tidal currents in some places have a highly kinetic energy associated that can be exploited. In this analysis the Advanced Circulation Model (ADCIRC) was applied to reproduce the coastal tidal circulation in the Lima estuary. This study began with a preliminary study of similar ADCIRC applications. Then an introduction to the ADCIRC model was made. The study proceeded with the model setup that involved a simplification in the bathymetry data in the shallower areas. The model calibration was made by comparison with records obtained during a measurement campaign in the field. This allowed choosing the more accurate parameters to describe the circulation observed. With the purpose of taking the real bathymetry, without simplifications, into account, an important feature from ADCIRC was considered in the next step: the wetting/drying tool. The consequences of the new approach were observed. Finally, the model was used to simulate three different scenarios. The first one allowed the assessment of tidal current energy since this scenario was forced only by the astronomic tides. The other two were scenarios for the recurrence interval of 5 and 100 years. The first scenario led to a conclusion about the energy potential of tidal currents after a research on that type of technology involving features and requirements.

1. ADCIRC model

This Finite Element Hydrodynamic Model created by Drs Rick Luetlich, North Carolina University and Joannes Westerink, Notre Dame University, was projected for coastal oceans, inlets, rivers and floodplains applications. The model is based on the solution of the generalized wave equation formulation

of the governing equations on a highly flexible unstructured grid. The basic equations in a geographic coordinate system are defined as follows:

$$\frac{\partial U}{\partial t} + \frac{U}{R \cos \phi} \frac{\partial U}{\partial \lambda} + \frac{V}{R} \frac{\partial U}{\partial \phi} - fV - \frac{UV \sin \phi}{R \cos \phi} = -\frac{g}{R \cos \phi} \frac{\partial(\zeta - \alpha \eta)}{\partial \lambda} - \frac{\tau_{bx}}{\rho_0 H} \quad (1)$$

$$\frac{\partial V}{\partial t} + \frac{U}{R \cos \phi} \frac{\partial V}{\partial \lambda} + \frac{V}{R} \frac{\partial V}{\partial \phi} + fU + \frac{UV \sin \phi}{R \cos \phi} = -\frac{g}{R} \frac{\partial(\zeta - \alpha \eta)}{\partial \lambda} - \frac{\tau_{by}}{\rho_0 H} \quad (2)$$

$$\frac{\partial \zeta}{\partial t} + \frac{1}{R \cos \phi} \frac{\partial(UH)}{\partial \lambda} + \frac{1}{R \cos \phi} \frac{\partial(VH \cos \phi)}{\partial \phi} = 0 \quad (3)$$

were t is time, λ and ϕ are the longitude and latitude (in degrees), ζ is the free surface elevation, U e V are the depth average-horizontal velocities, $H = \zeta + h$ is the water column depth, h is the bathymetric depth, f is the Coriolis parameter, ρ_0 is the reference density, g is the gravitational acceleration, α is the Earth elasticity factor, η is the Newtonian equilibrium tidal potential, τ_x and τ_y are bottom stresses in x and y directions.

These base equations are projected onto a planar surface using a Carte Parallelogramatic Projection in order to account for the Earth's curvature in the finite element discretization. The resultant equations associated with the generalized wave continuity equation (GWCE) which is expressed below in CP coordinate system are the ones that are finally solved by the ADCIRC model [1].

$$\begin{aligned} \frac{\partial^2 \zeta}{\partial t^2} + \tau_0 \frac{\partial \zeta}{\partial t} + \frac{\cos \phi_0}{\cos \phi} \frac{\partial}{\partial x'} \left[U \frac{\partial \zeta}{\partial t} - \frac{\cos \phi_0}{\cos \phi} UH \frac{\partial U}{\partial x'} - VH \frac{\partial U}{\partial y'} + \frac{\sin \phi}{R \cos \phi} UVH + fVH - gH \frac{\cos \phi_0}{\cos \phi} \frac{\partial(\zeta - \alpha \eta)}{\partial x'} - \left(\frac{\tau_{bx}}{\rho_0 H} - \tau_0 \right) UH \right] + \\ + \frac{\partial}{\partial y'} \left[V \frac{\partial \zeta}{\partial t} - \frac{\cos \phi_0}{\cos \phi} UH \frac{\partial V}{\partial x'} - \frac{\sin \phi}{R \cos \phi} \frac{\partial(\zeta - \alpha \eta)}{\partial x'} - \left(\frac{\tau_{bx}}{\rho_0 H} - \tau_0 \right) VH \right] - \frac{\partial}{\partial t} \left(\frac{\sin \phi}{R \cos \phi} VH \right) - \tau_0 \frac{\sin \phi}{R \cos \phi} VH = 0 \quad (4) \end{aligned}$$

At each simulation, the ADCIRC model gives the water surface elevation and the velocity field in the domain.

2. Model setup to the Lima estuary

Lima estuary

The Lima river has its source in the Spanish province of Galicia, crosses the north of Portugal and reaches the Atlantic ocean in the city of Viana do Castelo. This estuary (shown in Figure 1) is a relatively wide but shallow basin with mudflats that become covered during the ebb. Since 1988 there were three major dredging works in this area removing about 2500 000 m³ of material. These operations were made to allow navigability from the entrance zone to the downstream of the Eiffel bridge.

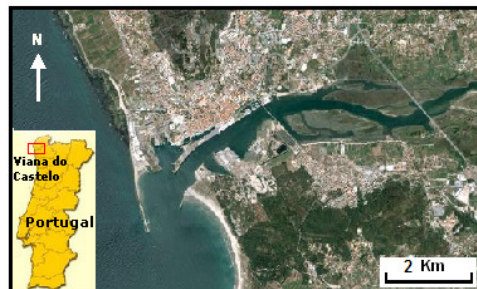


Figure 1: Lima estuary.

Model bathymetry

The bathymetry data used in this model came from a previous study in the same area. The ADCIRC model can work with both coordinate systems (cartesian or geographic). For the present study the geographic system was chosen. This option makes it possible to use the tidal harmonic constituents in the ADCIRC's database to define the ocean boundary condition. The bathymetric data was converted to the desired system referenced to the WGS 1984 ellipsoid and it was referenced to the local mean sea level. Due to the relative small size of some docks in the estuary zone, some of those structures were left out of the model domain. The consideration of these docks would require the existence of tiny elements in order to describe them well and this would add an unnecessary complexity to the mesh and constrains the time step of the model.

Model mesh

This fundamental component establishes a connection between the bathymetry configuration and the way the computer calculations are solved. The ADCIRC model works with unstructured meshes comprising triangular elements. It uses the finite element method to solve the intervenient differential equations. The quality of the mesh is an important issue because it leads to a better model stability and to more accurate results. The mesh created for this domain was built based upon two adjacent polygons. The first polygon includes the ocean area to the estuary entrance. This mesh has an element graduation consistent with the depth, meaning that the ocean elements are big and the ones near the coast are small. It was forced that the elements decrease their size as they get closer to the estuary entrance. The second polygon comprises the rest of the domain in the river zone for 20 km approximately. In this zone the mesh has small elements with a more constant size. The final mesh (Figure 2) resulted through the merging of both meshes. It has 10 706 elements, 6039 nodes, a minimum grid spacing of 22,2 m and a maximum grid spacing of 795,5 m.

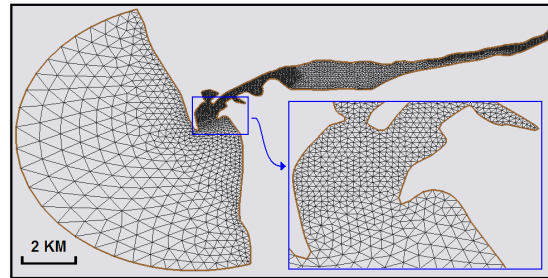


Figure 2: Finite element mesh for the Lima

Bottom stress

Three different formulations can be applied to the bottom stress. These can be constant or variable in space. This parameter is defined by:

$$\tau_{bx} = U \tau_* \quad \text{and} \quad \tau_{by} = V \tau_* \quad (5)$$

And the friction term, τ^* , can be expressed in a linear formulation (6), in a quadratic formulation (7) where C_f is a constant value, or in a hybrid formulation (8) where C_f is expressed by the equation (8)

$$\tau_* = C_f \quad (6) \quad \text{and} \quad \tau_* = \frac{C_f (U^2 + V^2)^{1/2}}{H} \quad (7)$$

$$C_f = C_{f \min} \left[1 + \left(\frac{H_{break}}{H} \right)^\theta \right]^{\lambda/\theta} \quad (8)$$

In the equation (8) $C_{f \min}$, H_{break} (wave breaking high), θ and λ are constant terms.

In the last formula the C_f approaches C_{fmin} in deep water, where $H > H_{break}$, and approaches $C_{fmin} (H_{break}/H)^\theta$ in shallow water, where $H < H_{break}$. The exponent θ determines how rapidly C_f approaches each asymptotic limit and λ determines how rapidly the friction coefficient increases as the water depth decreases.

The quadratic bottom stress formulation, with $C_f \sim 0,0025$, is the recommended for the major part of the coastal simulations. On the other hand, the hybrid equation is recommended in domains with shallow waters, specially, when wetting/drying is considered. The three bottom stress formulations were experimented. The best results were obtained using the hybrid and the quadratic formulation. There was an attempt to use the recommended values of C_f in both formulations but that value led to unstable simulations which crashed before the end. The best values used were $C_f = 0,004$ in both formulations.

Ocean boundary condition

This condition can be defined by using an ADCIRC feature that imports the tidal harmonic constituents from an internal database (LeProvost database) which associates up to thirteen tidal constituents to the geographic nodes that belong to the ocean's boundary. Simulations using the ADCIRC database with five tidal harmonic constituents (K_1 , M_2 , N_2 , O_1 and S_2) and using all thirteen available constituents (M_2 , S_2 , N_2 , MU_2 , K_2 , T_2 , L_2 , $2N_2$, K_1 , O_1 , P_1 , Q_1 and NU_2) were tested. Another experiment was to force the model with the introduction of the tidal sinusoidal curve built with the Tidal Table values. Simulation showed that the use of all tidal constituents available in the database led to the most accurate results. The introduction of the Tidal Table curve turned out to be a slightly better option when compared with the use of only five tidal constituents.

Upstream boundary condition

Naturally it is assumed that there is a flow in Lima river which can affect the study zone. Consulting the *Sistema Nacional de Informação de Recursos Hídricos* (SNIRH) site to the closest available hydrometric station (*Ponte da Barca*) the instantaneous flow for the simulation's period was found. The river flow is usually very small and the highest values are due to the discharges that come from the Touvedo's dam that controls the flow turbinated from a dam upstream. Therefore it was decided to adopt a constant value to define the river flow. The SNIRH site provided the average flow value in October: $34,97 \text{ m}^3/\text{s}$. This value was introduced in the model with an initial ramp period. The simulation with that flow improved the results, when compared with a simulation that does not consider any river flow.

Time-step

The time-step is related to the model stability and its appropriated selection is crucial to the total computational time. It is possible to determine a maximum value to this parameter applying the Courant-Friedrich.Levy (CFL) condition:

$$Cr = \frac{\sqrt{gh}\Delta t}{\Delta x} < 1 \quad (9)$$

where Cr is the Courant Number, g is the gravitational acceleration (m/s^2), h is the depth in each node (m), Δt is the time-step (s) and Δx represents the element size (m).

As shown, this condition is linked with the mesh: the bigger the mesh resolution, the smaller the time-step must be. A time-step of 2 s was used.

Calibration of the simplified model

For this calibration phase a bathymetry simplification was made assuming that all the shallow zones have a minimum depth of 1 m. The ADCIRC's simulations started in October 3rd, 2006, at 9 p.m. (in a flood phase) and had the duration of twelve days.

The calibration was made by comparing the results obtained with the observed data supplied through a measurement campaign by Compass Hydrographic Services Ltd[2] providing measurements at four sites (Figure 3) in the Lima river over a portion of the Spring Neap cycle. This campaign occurred in October of 2006. The data was adjusted in order to account for the atmospheric pressure fluctuations. Therefore, the values compared refer to the astronomic tidal only. The water surface elevation and the magnitude and direction of the velocity vectors were the compared variables. The instrument gauge positioned at Site 2 was accidentally disrupted by a local fisherman compromising these measurements results.



Figure 3: Tide gauges sites.

It was also possible to compare the water surface elevation in a site at the entrance of the estuary where Viana do Castelo's tide gauge is located.

The results obtained represented the water levels well. However an ascendant lack of precision in the more upstream sites was noted. The velocity results weren't as good as the levels. Still in general they represented the ebb-flood asymmetry well.

3. Wetting/drying

The tidal circulation in the estuary in a more authentic way was obtained by considering the real bathymetry data and with the observed sand banks and mudflats in the middle of the domain. In order to do that the wetting/drying tool was applied. This function comprises an algorithm that assumes the wet and drying of the elements in the mesh. Each node of the mesh is defined as dry, interface or wet node. According to its node's connection, each element can also be considered as dry or wet. [3]. The assessment for each node is made with reference to a minimum wetness height, H_{min} , which can be defined by the user. The user can also define the number of time steps that a node has to remain wet before it can be turned off and the minimum time-step in dry conditions. In addition the user can define a minimum velocity, V_{min} , which has to be checked during the wetting/drying node passage [4]. In this model a value of 0,05 for H_{min} was used, a minimum value of twelve time-step for wet and for dry conditions and a V_{min} equal to 0,05 m/s.

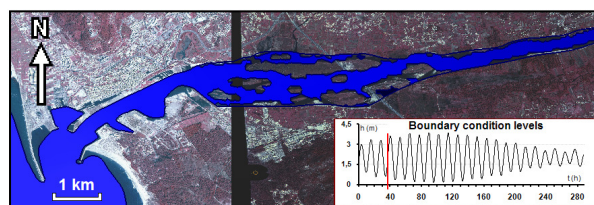


Figure 4. Water circulation in a flow phase using wetting/drying.

Due to stability constraints a time-step of 0,25 s and a value of 30 for the lateral viscosity were used. These problems led also to a reduction in the mesh extension comprising now 8 322 elements and 4 649 nodes. In this simulation the best parameters chosen in the last section, with $C_r = 0,0025$, were used. Figure 4 shows an instant of the simulation with wet and drying.

4. Comparison with measured currents

The wetting/drying model supplied the best results with the improvement, especially, of the velocity results. Figure 5 show the result of the water surface elevation and of the comparisons made for the Viana do Castelo's tide gauge and for the most upstream site (Site 4). Figure 6 shows the velocities magnitude comparisons.

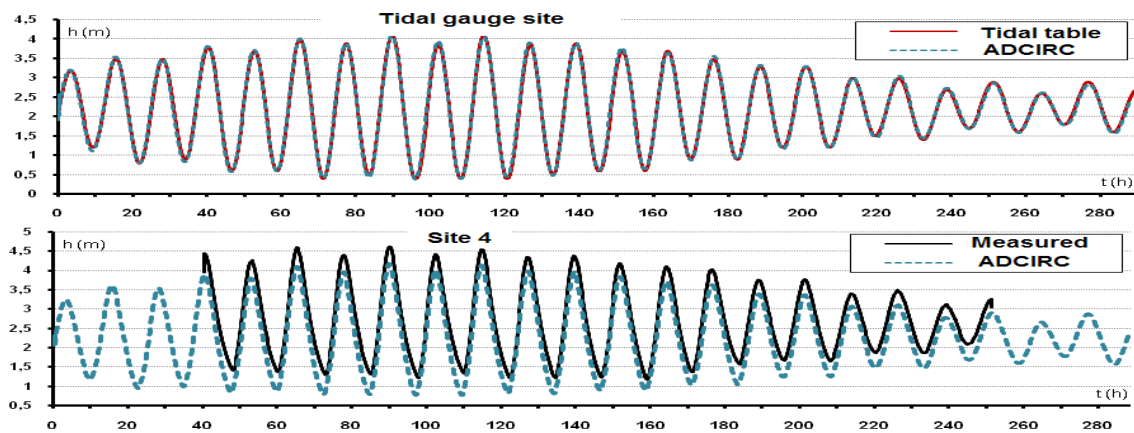


Figure 5. Water surface elevations with wetting/drying.

As it happened with the results during the calibration phase the water level shows a good representation. However with the wetting/drying a slight improvement in the description of Site 4 is noted.

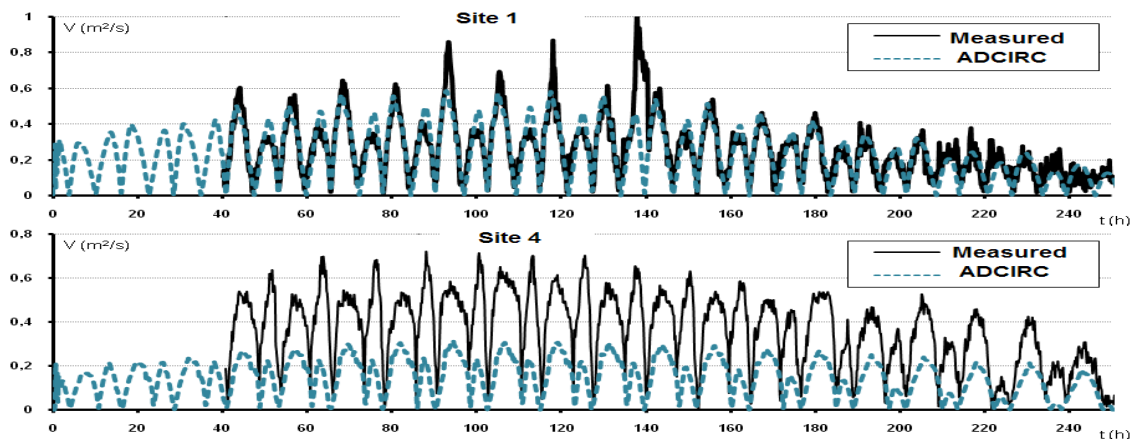


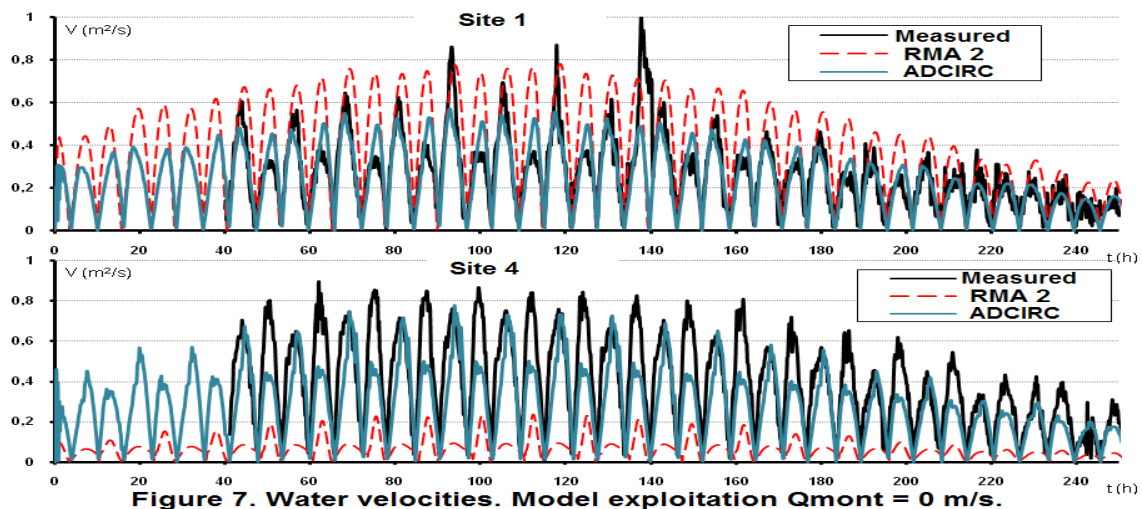
Figure 6. Water velocities with wetting/drying

Now the velocity magnitude presents a value's scale which is almost coincident with the data observed in Site 1 and 3. It is also detected that the simulated ebb-flood asymmetry is contrary to the measurements in Sites 3 and 4.

The results of the direction of the velocity vector show that the model also properly describes the physics and is in accordance with what was expected in each site. These values demonstrate differences of direction of 180° that correspond to a total reverse inversion of the circulation direction in the ebb and flood cycle.

5. Model exploitation

The model built was used to simulate a scenario that could lead to the appropriated assessment of the tidal energy potential. Consequently, for this analysis only the tidal part in the water motion matters, neglecting the river flow and the atmospheric effects. These results were compared with the observed data and with results obtained in *Teixeira (2006)*[5] (that neglected the wetting/drying option by forcing the bathymetry to have a minimum depth equal to the mean local sea level). Considering the water levels obtained in both models, ADCIRC and RMA2 describe the phenomenon's physics in an accurate way. In Site 3 the ADCIRC demonstrated a slight improvement when compared to the RMA2. It is shown in Figure 7 the velocity comparisons made in the Site 1 and Site 3



Observing the velocity magnitude values it is clear that the ADCIRC has a better capacity to reproduce the measured values and that the wetting/drying feature is important for the results of Site 3.

The model's ability to simulate an extreme situation was also tested. The results were compared with the results in *Teixeira, (2006)*. Two simulations for two different scenarios were made, for the recurrence interval of 5 years and 100 years. A flood pick discharge value of $1900 \text{ m}^3/\text{s}$ and $4200 \text{ m}^3/\text{s}$ it was used respectively. It was possible to observe that the results in Site 1 and 2 don't show as notorious differences as the ones in Site 3, in terms of level and velocity's results. In Site 3 the water level simulated with ADCIRC presented lower values and more accentuated oscillations indicating a more intense tidal influence. Concerning the velocity values in Site 3, ADCIRC shows again bigger oscillations with higher magnitude values.

6. Tidal energy

The most traditional known tidal energy production method is performed using the difference in elevation of the tide during the ebb and flood. It involves the building of a dam in estuary zones, allowing the water to fill a reservoir. When the water level starts to decrease the floodgate is shut and the water is retained containing potential energy. Afterwards the water can flow to the sea activating the turbines and producing energy. Since the 60's, the biggest model of these tidal dams is in the river Rance, in France. This method denotes a difficulty in providing a regular energy and is only feasible in places where the tides have amplitudes higher than 5,5 m. The investment that has to be made to build the dam is high. So is the construction period. And, since the production factor of the system is low this leads to long investment

return periods. Another disadvantage in this technique is the inconvenient environmental impact on the local ecosystems. All these particularities add a non-competitiveness factor to this system[6].

For a few decades a more attractive method to produce energy from tides has been developed. It consists in a system that captures the kinetic energy within the constant movement of the tidal fluxes. The energy production is obtained through the use of tidal turbines installed underwater. Due to the higher water density, when compared with the air, these tidal turbines can generate the same energy as a wind turbine although requiring lower fluid velocities and smaller areas. The tidal systems have associated a much more accurate forecasting than wind systems can have. The tidal turbines have the advantages of having an easy installation; the visual impact is minor; they don't cause significant danger to the sea life and there can be navigation around the installation zone. On the other hand, these turbines face some problems that may be solved in the future, like the strong drag forces in contact with the structure; the development of plants on top of the blades; corrosion; storm damages and in some places they can restrict navigation.

Many different tidal turbines systems are offered. For example, they can differ in features like rotation axis (vertical or horizontal), the rotor (with or without a duct) or the type and number of blades. The mooring systems can be a gravity base, mono-pile, piled-jacket and floating. The first two are recommended for shallow waters.

There is another type of equipment that uses the tidal fluxes kinetic energy to produce energy but doesn't present the same rotational movement as the turbines. These systems operate through a linear vertical movement in a hydrofoil element induced by the current flow. Two systems of this kind are shown in Figure 8, the Stringray from The Energy Business Lda and the Sea Snail.

As an example, some tidal turbine developers are listed and shown in Figure 8 : Seaflow from the Marine Current Turbine Ltd, TidEl from SMS Hydrovision, Lunar System from Lunar Energy Ltd, Verdant Power, Clean Current, Open Hydro and Nereus from Atlantis Resources Corp, Kobolt Turbine from Enermar, Ponti Di Archimede SpA, Davis Hydro Turbine from Blue Energy and Gorlov Turbine.

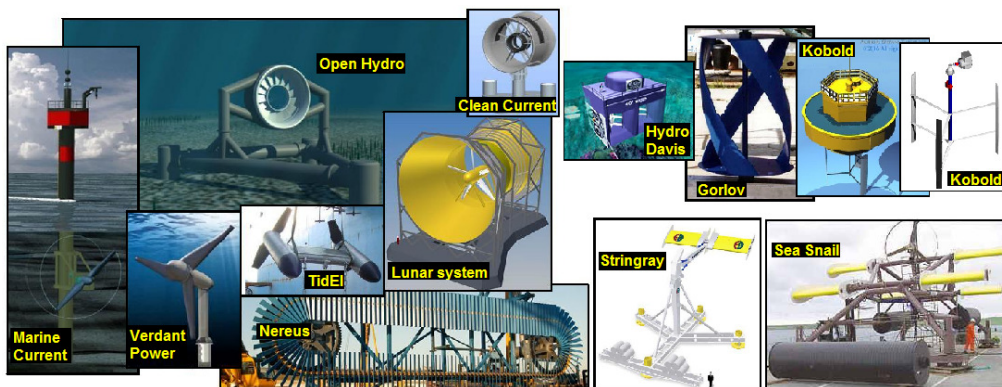


Figure 8. Tidal current energy systems.

In general, systems can be found that require velocities between the 0,5 m/s and 6 m/s and the recommended velocities are around 2 m/s. The systems also require a water depth that goes from 9 m up to 50 m.

This study considers the application of a tidal current kinetic energy system. Therefore it is important to now that the power available in a water flux in a section is:

$$P = 1/2 \rho \int_A V^3 dA \quad (10)$$

were ρ is the sea water density, A is the section and V the flow velocity.

And, the power that can be extracted by a tidal energy equipment is:

$$P_t = 1/2 \eta \rho A_t V^3 \quad (11)$$

were η is the equipment efficiency and A_t is the effective area of the turbine.

Hence, the turbine potential is correlated with the dimension, efficiency and depends heavily on the velocity of the tidal current.

7. Tidal assessment in the Lima estuary

The equation (10) shows that the sites with higher current velocities are the most favourable site for the installation of a tidal system. The detection of the site with more potential was made by also taking into account the local bathymetry depth. The bathymetry referring to the mean sea level in the estuary is shown in Figure 9.

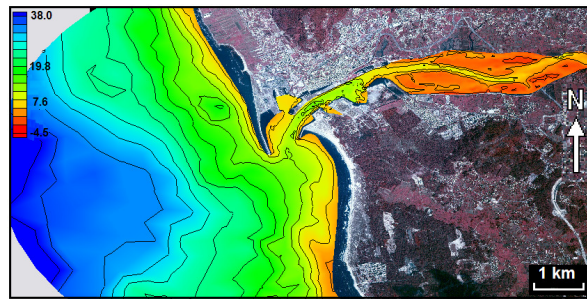


Figure 9. Bathymetry in the Lima estuary.

Through the simulation it was detected that the velocities during that period ranged between 0 and 1,34 m/s. Despite of these low values six sites to evaluate the local values were chosen. These sites are shown in Figure 10 also with the velocity field during a flood phase.

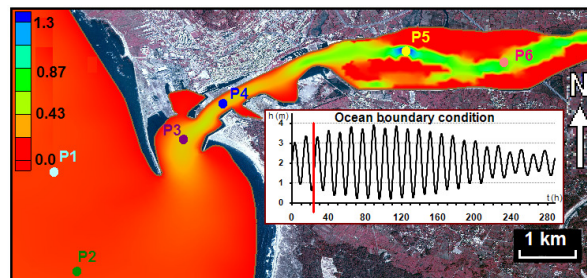


Figure 10. Velocity field in a flow phase.

The values found in those places are expressed in Table 1.

It was observed the sites P1 and P2 have really low velocities; therefore the option of installing any tidal equipment is unfeasible. Sites P3 and P4 also have insufficient current velocity and since those sites are located in the estuary zone with had dredging works to guarantee navigability, the installation on the tidal energy structures is not possible without ruining the navigational channel. Sites P5 and P6 have the highest velocities, however their depth doesn't seem to be sufficient for the installation of tidal energy systems. Yet, in site P5 the situation could be reconsidered in the future: the installation of a tidal system like the Blue energy turbine that can associate elements forming a fence across the channel in order to use part of all the section flux available in the site.

Site	Depth (m)	Velocity (m ³ /s)		
		Average	Máx.	Mín.
P 1	20,3	0,037	0,090	0,001
P 2	25,2	0,037	0,085	0,001
P 3	7,2	0,147	0,425	0,002
P 4	12,2	0,154	0,412	0,000
P 5	4,5	0,380	1,297	0,000
P 6	3,9	0,227	0,573	0,000

Table 1. Velocities in the analysed sites.

8. 7 Final considerations

At the end of the paper a crucial importance is given to the previous research phase that supplied essential information about similar studies with the ADCIRC model. This helped on the model construction especially in the difficult phase that occurred in the wetting/drying consideration.

In the calibration phase, the maximum number of tidal constituents which were used to force the model was the available in the ADCIRC's database. However it is known that in order to obtain more accurate tidal wave simulations, the maximum tidal constituents available from different databases should be used and the errors associated to these constituents should also be considered.

The results which were obtained elucidated the significance of the wetting/drying tool, especially to describe the water circulation in the shallow zone of the Lima estuary. Still it was confirmed that a bathymetry simplification in order to simulate the estuary zone downstream the Eiffel bridge is acceptable.

Finally, the conclusion which can be drawn is that the analyzed domain doesn't demonstrate a hydrodynamic favourable to the installation of the equipment that exists today. The estuary is characterized by low current velocities, low amplitude differences and a shallow bathymetry. Nevertheless, with the development the tidal energy equipment, it may be possible to look at sites like site P5, with new and favourable perspectives relating the energy production.

Acknowledgements

The initial data used in the model developed during this thesis was converted to a geographic coordinate system by *Secção de Sistemas de Apoio ao Projecto do Instituto Superior Técnico*.

References

[1] JAROSZ, Ewa. *TIDAL DYNAMICS IN THE BAB EL MANDAB STRAIT*. A Dissertation Submitted to the Graduate Faculty of the Louisiana State University and Agricultural and Mechanical College in partial fulfilment of the requirements for the degree of Doctor of Philosophy. M.S., Louisiana State University, 1997.

[2] HIDRODATA, Consultores de Hidrografia e Oceanografia, Lda. *Relatório Levantamento Topo-Batimétrico, Campanha de Medição de Correntes e Níveis e Recolha de Amostras*. Outubro/Novembro de 2006.

[3] AGGARWA, Manish. *STORM SURGE ANALYSIS USING NUMERICAL AND STATISTICAL TECHNIQUES AND COMPARISON WITH NWS MODEL SLOSH*. A Thesis Submitted to the Office of Graduate Studies of Texas A&M University in partial fulfilment of the requirements for the degree of MASTER OF SCIENCE. Agosto, 2004.

[4] DIETRICH, J.C.; KOLAR, R.L.; LUETTICH, R.A., 2004. *Assessment of ADCIRC's Wetting and Drying Algorithm* - School of Civil Engineering and Environmental Science, University of Oklahoma, Norman, 73019.

[5] TEIXEIRA, António Trigo *PONTE EIFFEL HIDRODINÂMICA do ESTUÁRIO DO LIMA. Estudo em Modelo Matemático* – CEHIDRO Grupo de Costas e Portos. Janeiro 2007.

[6] TAVARES, Walter Marques, *PRODUÇÃO DE ELECTRICIDADE A PARTIR DA ENERGIA MAREMOTRIZ* – Consultoria Legislativa Anexo III Março 2005.